Indian Journal of Chemistry
Vol. 62, May 2023, pp. 518-526
DOI: 10.56042/ijc.v62i5.1451

An effective colorimetric and fluorescent chemosensor derived from modified curcumin for the detection of the Fe^{3+} ion

Pappian Rajam & Rajaram Mahalakshmy*

Department of Chemistry, Thiagarajar College (Affiliated to Madurai Kamaraj University), Madurai 625 009,
Tamil Nadu, India
*E-mail: mahalakshmy_chem@tcarts.in

Received 12 January 2023; accepted (revised) 23 March 2023

From curcumin and 1-aminonaphthalene, the chemosensor NIBMP (4,4'-(3,5-bis(naphthalene-1-ylimino)hepta-1,6-diene-1,7-diyl)bis(2-methoxyphenol)) has been prepared. For Fe^{3+} as opposed to other metal ions, NIBMP serves as both a colorimetric and a fluorescence turn-off sensor. Interactions between NIBMP and Fe^{3+} reveal a noticeable colour shift from yellow to brown. The absorption and fluorescence studies reveal new peaks at 326 nm and quenching at 530 nm, respectively. The limit of detection, 0.139 µM, is found to be significantly lower than the EPA's standard for drinking water (5.37 µM). There is evidence for a 1:1 stoichiometry between NIBMP and Fe^{3+} utilizing Job's plot analysis and ESI-HRMS. Additionally, a Stern-Volmer plot has been created, and its quenching constant has been computed. Moreover, EDTA's fluorescence analysis has been used to test whether the complexation of NIBMP with Fe^{3+} is reversible. Significantly, Fe^{3+} is successfully detected using NIBMP in actual water samples with excellent recoveries.

Keywords: Fluorescence, 1-Aminonaphthalene, Schiff base, Curcumin, Colorimetric

Most biological and environmental systems depend greatly on metal ions. Without trace amounts of metal ions like vanadium, molybdenum, cobalt, copper, iron, manganese, nickel, chromium, and zinc, all organic systems would not work properly[1]. All living things are dependent on iron, which is the most abundant element on earth and required for oxygen transfer, DNA synthesis, and electron transport[2]. Similar to this, too much or not enough iron may lead to a variety of issues, including hemochromatosis, anaemia, heart disorders, metabolic acidosis, hypovolemic shock, damage to the liver and brain, and stomach discomfort, nausea, and vomiting[3]. Additionally, it contributes to Parkinson's and Alzheimer's diseases[4]. Sensing this ion has become crucial because of the consequences that iron, in particular, has on biological and environmental systems. Therefore, it is crucial to identify and detect iron using straightforward, affordable, highly selective, and sensitive technologies. In this regard, colorimetric and fluorescent technologies are superior to other types of metal ion detection due to its non-destructive nature, cheap cost, excellent sensitivity, and ease of target ion monitoring. For detecting Fe^{3+} ions, a number of colorimetric and fluorescent turn-on and turn-off mechanistic probes have been developed[5]. Even though there are several chemosensors for sensing metal ions, a simple, efficient, and environmentally friendly sensor for Fe^{3+} is still needed. Schiff base ligands, which include chromophore and fluorophore are attractive sites for optical sensing of metal ions, stand out from other chemosensors due to their simplicity in synthesis[6]. Thus, several scientists created curcumin-derived Schiff bases and curcumin analogues for the manufacture of metal complexes[7] and investigated their biological characteristics, including their (antibacterial, antimicrobial, anti-inflammatory, and anti-cancer). The yellow pigment known as curcumin, which has the chemical formula 1,7-bis-(4-hydroxy-3-methoxyphenyl)-1,6-heptadiene-3,5-dione, is derived from the roots of the Curcuma longa plant. It combines with primary amines to generate a Schiff base ligand. Numerous curcumin and curcumin analogues have been studied for use in sensing applications[8,9]. In this way, a curcumin-derived Schiff base ligand was employed to identify metal ions.

In this study, curcumin and 1-aminonaphthalene were combined to create a Schiff-base based chemosensor (NIBMP). Imine groups in the produced ligand served as an ion receptor for Fe^{3+}. Studies on naked eye detection, absorption, and emission were conducted as a consequence of NIBMP's ability to preferentially perceive Fe^{3+} above other recycled metal ions. The addition of Fe^{3+} caused the visual color to shift from yellow to brown, the strength of NIBMP's absorption to decrease, and the fluorescence quenching mechanism, which may be the result of NIBMP complexing with Fe^{3+}.

Experimental Section

All the analytical quality chemicals utilised in this experiment were obtained from commercial suppliers, and used as such without any further purification. Metal solutions of Na^{+}, Ca^{2+}, Mn^{2+}, Fe^{2+}, Fe^{3+}, Co^{2+}, Ni^{2+}, Cu^{2+}, Zn^{2+}, Cd^{2+}, Al^{3+}, Hg^{2+}, Sn^{2+}, Pb^{2+} and sodium salts of anions were made from their chloride salts in pure ethanol.

Jasco FP-6200 spectrofluorometer and Jasco V-530 spectrophotometer were used to examine the sensor's optical characteristics. A Bruker Advance III HD Nanobay 400 MHz FT-NMR spectrometer was used to record the ^{1}H NMR spectra of NIBMP in deuterated dimethyl sulphoxide (DMSO-d_6). Acetonitrile was used as the solvent for the liquid chromatography-mass spectrometry (LCMS) and high-resolution mass spectrometry (HR-LCMS) measurements, while the FT-IR spectra were captured using a Shimadzu FTIR-8400S instrument in the 4000-400 cm^{-1} range with KBr pellets.

Synthetic procedures

Synthesis of NIBMP

With modest modifications to the existing approach, NIBMP was synthesised in a single step using the method described here[10]. Using a magnetic stirrer, curcumin (0.368 g, 1 mmol) was dissolved in ethanol at 60°–70°C. A catalytic quantity of acetic acid and 1-aminonaphthalene (0.286 g, 2 mmol) in ethanol were gradually added to the agitated solution. Using an oil bath, the solution was allowed to reflux for 6 h at 70°C to 80°C. Thin-layer chromatography was used to track the reaction's development. After obtaining a dark liquid, the surplus solvent was finally eliminated using a rotary evaporator operating at decreased pressure. Finally, after drying, hexane washing, and ethanol recrystallization, a reddish-brown precipitate was obtained. Further research has made use of the recrystallised product.

Preparation of NIBMP-$M^{2+(or)3+}$ complex

All the **NIBMP-$M^{2+(or)3+}$** complexes were synthesized *in situ* in the molar ratio of 1:1 (metal: ligand).

Preparation of NIBMP-Fe^{3+} complex

An ethanolic solution of $FeCl_3$ (1 mmol), the ligand NIBMP (1 mmol), and catalytic amounts of triethylamine were stirred for around 5 h at RT to prepare the complex NIBMP-Fe^{3+}. The result was a dark brown precipitate, which was filtered before being rinsed with ice-cold ethanol and water and dried.

Colorimetric and Fluorescence studies

Preparation of the ligand NIBMP and metal ion solutions

In ethanol, a stock solution containing the metal ions Na^{+}, Ca^{2+}, Mn^{2+}, Fe^{2+}, Fe^{3+}, Co^{2+}, Ni^{2+}, Cu^{2+}, Zn^{2+}, Cd^{2+}, Al^{3+}, Hg^{2+}, Sn^{2+}, Pb^{2+} and anions such as NO_3^{-}, PO_4^{3-}, CrO_4^{2-}, CO_3^{2-}, Cl^{-}, CH_3COO^{-} was prepared. A 10 μM solution of the relevant metal solutions and a 1 μM solution of the sensor were combined in a 3 mL cuvette for colorimetric and fluorescence investigations. The range of the absorption wavelength was 200 to 800 nm.

Selected experimental procedures

Through measurements of absorbance and fluorescence spectrum changes as well as changes in colour visible to the naked eye, the selectivity of the sensor NIBMP towards different metal ions was examined. A 1 μM solution of the sensor received 10 μM metal ions as an addition. The sensor's readings of the absorbance, fluorescence, and colour changes of several metal ions were assessed.

Absorbance and fluorescence titrations

The results of absorbance and fluorescence titrations were used to illustrate the sensor's sensitivity to Fe^{3+}. In the absorbance titration experiment, a constant volume (1 μM) of the sensor was filled with solutions containing varying concentrations of the metal ion Fe^{3+} in regular intervals, and the changes in absorbance were recorded. Similar to this, 1 μM of NIBMP was used in the fluorescent titration experiment. A 1-38 μM solution of Fe^{3+} ion was introduced progressively, and variations in the fluorescence intensity were noted.

Job's plot measurements

Overall combined concentration of NIBMP and Fe^{3+} ion in each of the NIBMP and Fe^{3+} in ethanol solutions was kept constant at 10^{-4} M throughout the preparation of the solutions. After shaking each solution for a short period of time, the produced solution was taken in a vial and diluted to a volume of 3 mL. The absorbance of each solution was then measured. Job's plot was made by plotting the greatest absorbance value obtained from a series of prepared solutions against the mole fraction of the metal ion. The maximum value of the Job's plot denoted the stoichiometric ratio of the metal with ligand in a complex.

Competitive binding experiments

Competitive binding experiments were used to assess NIBMP's affinity for Fe^{3+}. Other metal ions were present at the same time as the absorbance was measured. Here, 10 µM of various metal ions and 10 µM of the Fe^{3+} ion were added individually to a 1 µM NIBMP solution. The findings demonstrated that even in the presence of competing metal ions, NIBMP preferentially recognises Fe^{3+}.

Effect of *p*H

The sensing ability of fluorescent sensor NIBMP to detect the presence of Fe^{3+} at various *p*H levels was examined using solutions of NIBMP (1 µM) in ethanol and Fe^{3+} salt solution (10 µM) With the use of a 0.1 mM NaOH and HCl solution, the *p*H range of 2–14 was adjusted.

Real sample analysis

The Cauvery River water used at home, as well as tap water from the Thiagarajar College campus and RO water, was all sampled. Filtration with Whatman No. 1 filter paper was used to get rid of the contaminants that were found in these samples. The pure water samples were then spiked with the NIBMP + Fe^{3+} combination, the absorbance changes were investigated, and recovery percentages were computed.

Results and Discussion

Synthesis and characterization

The ligand NIBMP was synthesized by condensation reaction of Curcumin and 1-aminonaphthalene in 1:2 ratio. All the metal complexes were synthesized *in situ* in the molar ratio of 1:1 (metal: ligand). The protocol used for the synthesis of NIBMP was depicted schematically in Scheme 1. All the synthesized compounds were characterized with different physiochemical and spectral techniques which provide evidence for their formation.

^{1}H NMR and Mass spectral studies

By using ^{1}H NMR and mass spectrometric analysis, the synthesized ligand NIBMP was characterized.

^{1}H NMR (DMSO-d_6, 400 MHz): δ 3.84 (s, 6H,-OCH_3), 5.7 (s, 2H-CH_2), 6.07 (s.1H-OH), 6.66-6.68 (d,=CH), 6.75 (d,=CH), 7.06-7.15(Phenyl protons) and 7.21-8.05(Naphthyl protons). ^{1}H NMR spectrum of NIBMP is given in Fig. S1.

HR-MS of NIBMP($C_{41}H_{34}N_2O_4$): *m/z* Calcd 618.25. Found 619.23[$M+H^+$]. Fig. S2 and Fig. S3 depict the HR-MS spectra of NIBMP and NIBMP-Fe^{3+} complex respectively.

IR spectral studies

We measured the FT-IR spectra of the NIBMP and NIBMP-Fe^{3+} combination. The FTIR spectrum of NIBMP is shown in Fig.S4. Based on the collected data, the phenolic -OH group of NIBMP was identified as the source of the weak wide band detected at 3284 cm^{-1}. The peak visible in the vicinity of 1625 cm^{-1} confirmed that there was unsaturation outside of the ring. The peak for the azomethine group was measured at 1574 cm^{-1}. The peak at 1000–1250 cm^{-1} proved the (C–O) bond's existence. The NIBMP's unique peak, which appeared at 1510 cm^{-1}, demonstrated that it was aromatically unsaturated.

The FTIR spectra of the NIBMP-Fe^{3+} complex was depicted in Fig. S5, and a wide band that was seen in the range of 3386 cm^{-1} correlated with the presence of the phenolic -OH group. At 1595 cm^{-1}, a prominent peak was visible that was distinguished by the presence of the azomethine group, which was at a higher wave number as a result of the complex's formation with Fe^{3+}. The presence of unsaturation was verified by a distinctive peak located at 1514 cm^{-1}.

Colorimetric and fluorescent studies

Na^+, Ca^{2+}, Mn^{2+}, Fe^{2+}, Fe^{3+}, Co^{2+}, Ni^{2+}, Cu^{2+}, Zn^{2+}, Cd^{2+}, Al^{3+}, Hg^{2+}, Sn^{2+}, Pb^{2+} and NO_3^-, PO_4^{3-}, CrO_4^{2-},

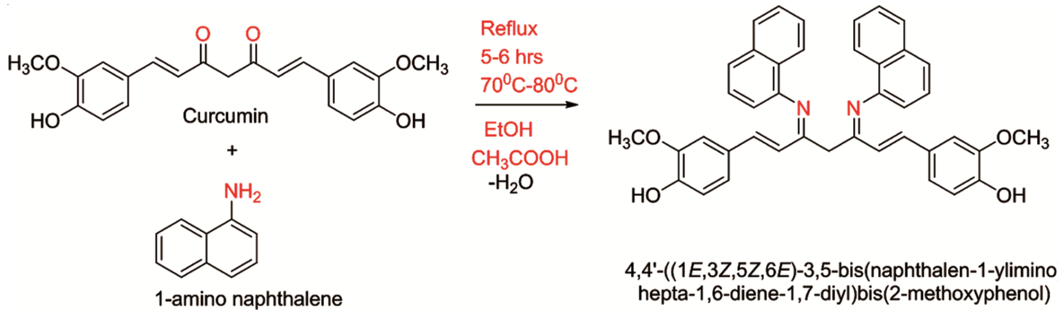

Scheme 1 — Synthesis of NIBMP

CO_3^{2-}, Cl^-, CH_3COO^- (10 μM) were used to examine colorimetric sensing of the NIBMP (1 μM) (Fig. S6a). With NIBMP, Fe^{3+} showed an apparent colour shift from yellow to reddish-brown; no other tested metal ions showed any appreciable colour changes that could be seen with the unaided eye. Fig. S6b demonstrated that Fe^{3+} significantly suppressed the yellow fluorescence that NIBMP exhibited under a fluorescent light as opposed to other metal ions. These findings demonstrated that the ligand NIBMP formed a compound and was sensitive to Fe^{3+}.

Absorbance and emission studies

In-depth optical experiments were conducted utilising UV-Vis and fluorescence methods based on the colorimetric data to investigate the selective sensitivity of NIBMP towards Fe^{3+}. The NIBMP absorption spectra in ethanol were examined with and without a number of metal ions (Na^+, Ca^{2+}, Mn^{2+}, Fe^{2+}, Fe^{3+}, Co^{2+}, Ni^{2+}, Cu^{2+}, Zn^{2+}, Cd^{2+}, Al^{3+}, Hg^{2+}, Sn^{2+}, $Pb^{2+}$and NO_3^-, PO_4^{3-}, CrO_4^{2-}, CO_3^{2-}, Cl^-, CH_3COO^-). The main chain of curcumin's π-π* transition was identified by NIBMP as having a maximum absorption wavelength at 423 nm (Fig. 1a)[11]. Additionally, a peak for the n-π* of the azomethine[12] moiety occurred at around 330 nm, and a very strong peak for the n-π* transition between the oxygen atom and the benzene ring appeared around 220 nm. Changes in absorbance were used to determine the selectivity of NIBMP towards different metal ions; except from Fe^{3+}, no particular changes in absorbance for metal ions were seen (Fig. 1b). After the addition of Fe^{3+}, there was a shift in the strength of NIBMP's absorption maximum, and a new peak was seen at 326 nm, demonstrating the selectivity of NIBMP towards Fe^{3+}(Fig. 1c).

Excitation wavelength of 423 nm was used in a fluorescence approach to determine the NIBMP's selectivity toward different metal ions. The free NIBMP released a sizable amount of intense yellow fluorescence at 530 nm. With the exception of Fe^{3+}, the presence of several metal ions (Na^+, Ca^{2+}, Fe^{2+}, Mn^{2+}, Fe^{3+}, Co^{2+}, Ni^{2+}, Cu^{2+}, Zn^{2+}, Cd^{2+}, Al^{3+}, Hg^{2+}, Sn^{2+}, Pb^{2+} and NO_3^-, PO_4^{3-}, CrO_4^{2-}, CO_3^{2-}, Cl^-, CH_3COO^-) did not significantly alter the fluorescence intensity of NIBMP (Fig. 2a).

But when Fe^{3+} was added to NIBMP, the fluorescence of NIBMP was only one-fourth as intense as it was in free form. The paramagnetic properties of Fe^{3+} and LMCT may be to blame for the fluorescence quenching of NIBMP with Fe^{3+} depicted in Fig. 2b.

Absorption and emission titration experiments

By using absorption and emission titration tests, the binding affinity of NIBMP with Fe^{3+} and detection limit were investigated.

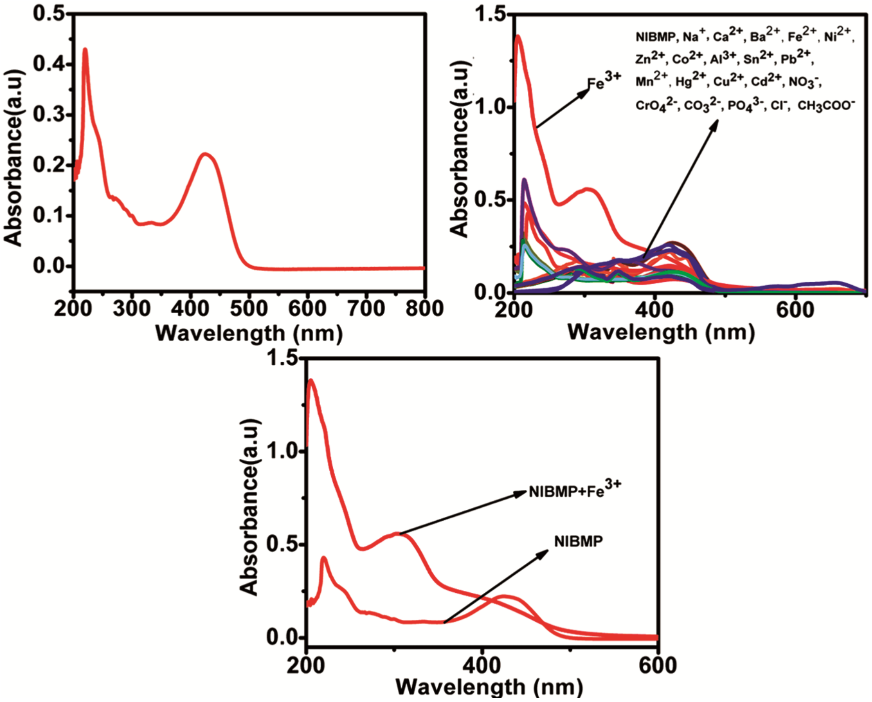

Fig. 1 — (a) UV-Vis Spectrum of NIBMP (b) UV-Vis spectrum of NIBMP with various metal ions (c) UV-Vis Spectrum of NIBMP with Fe^{3+}

The fluctuation in NIBMP (1μM) absorbance after adding Fe^{3+} ions (0–10μM) successively was depicted in Fig. 3a. With each subsequent rise in the concentration of Fe^{3+}, there was a steady drop in the intensity of the absorption maxima centered at 423 nm and an increase in the intensity at 326 nm and 220 nm. The creation of a new charge transfer complex between Fe^{3+} and NIBMP was revealed by the appearance of an isobestic point at 406 nm. Fig. 3b demonstrated a strong linear relationship between absorbance and Fe^{3+} concentration ($R^2 = 0.9927$). As a result, utilising 3σ/k, the detection limit of Fe^{3+} was established to be as low as 0.139μM. Where S represents the slope of the calibration curve and σ denotes the standard deviation of the blank solution. The absorbance titration experiment's linear plot provided the slope value. The resulting Fe^{3+} detection limit was substantially lower than the 5.37μM EPA drinking water guidelines[13].

Similar to this, a fluorescence titration experiment was conducted to determine the sensitivity of the sensor NIBMP towards Fe^{3+}. In this experiment, Fe^{3+} was added incrementally up to a concentration of 38 μM, which gradually reduced the luminous

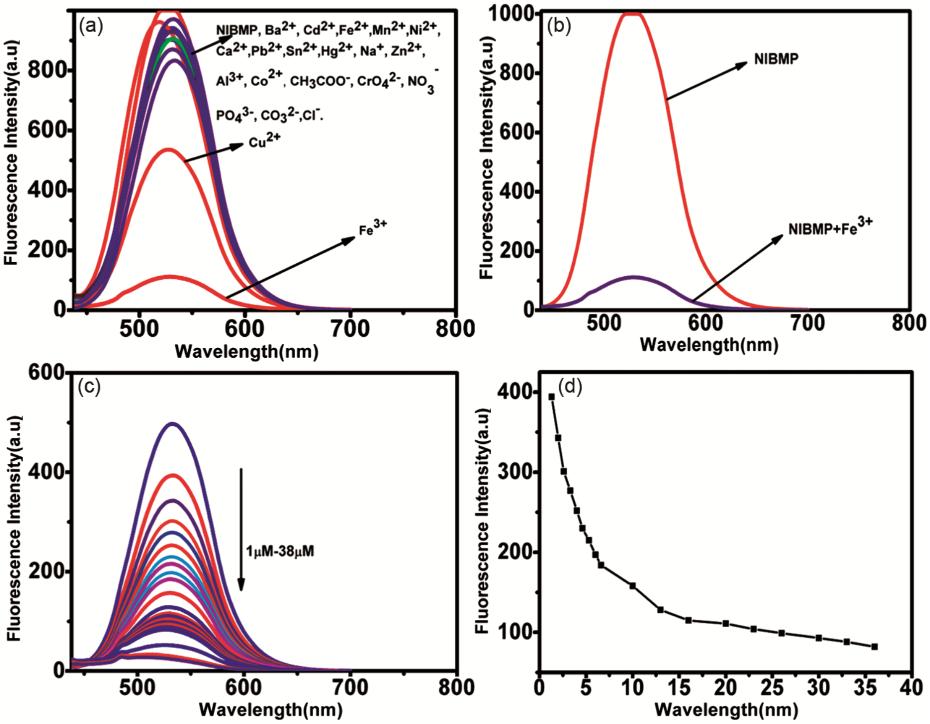

Fig. 2 — (a)Fluorescence spectrum of NIBMP with the addition of various metal ions (b) Fluorescence spectrum of NIBMP and NIBMP with Fe^{3+} (c) Fluorescence spectral changes of NIBMP upon addition of different concentrations of Fe^{3+} (1–38μM) (d) Fluorescence emission intensity of NIBMP as a function of $[Fe^{3+}]$.

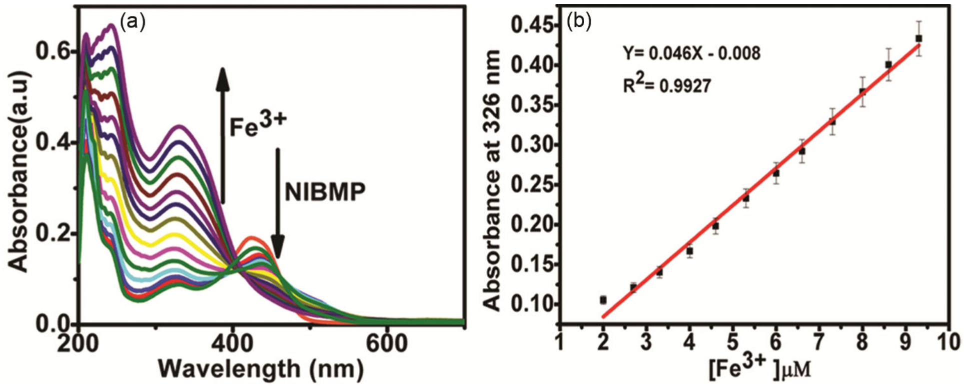

Fig. 3 — (a) UV–Vis. spectral changes of NIBMP upon addition of different concentrations of Fe^{3+} (1-10 μM). (b) Absorbance changes of NIBMP at 326 nm as a function of $[Fe^{3+}]$

intensity (Fig. 2c and Fig. 2d). Additionally, Fig. 4a demonstrated the linearity between fluorescence intensity and Fe^{3+} concentration, demonstrating the suitability of the ligand NIBMP for detecting Fe^{3+} ($R^2 = 0.9899$).

Additionally, the Stern-Volmer relation $F_0/F = 1 + Ksv[Q]$, where F and F_0 are the fluorescence intensities of NIBMP with and without Fe^{3+} ions, respectively, Ksv is the Stern-Volmer quenching constant, and [Q] is the concentration of Fe^{3+} ion, was employed to evaluate the Fe^{3+} ions' effectiveness in quenching. The Stern-Volmer constant $K_{SV}=3.27 \times 10^5 M^{-1}$ was computed using the Stern-Volmer (SV) plot[14] (Fig. 4c).

Effect of *p*H on Fluorescent studies

The *p*H was improved to better understand the sensor NIBMP's actual applicability. Using NaOH and HCl solutions, the *p*H was changed to examine the impact of *p*H variation on fluorescence studies of NIBMP with Fe^{3+}(Fig. 4b)[15]. Under acidic *p*H, the fluorescent intensity of the NIBMP - Fe^{3+} was strong; fluorescence quenching was noticed in the *p*H range of 7; and above *p*H 7, it remained steady. These findings demonstrated the ability of this NIBMP to bind to Fe^{3+} at neutral and basic *p*H levels.

Detection of stoichiometry

The molar ratio of the Fe^{3+} ion was changed to determine the binding stoichiometry of NIBMP with Fe^{3+} ($[Fe^{3+}]/([NIBMP] + [Fe^{3+}])$=0.1, 0.2, 0.3, 0.4, 0.5, 0.6, 0.7, 0.8, 0.9, 1.0). The total concentration of NIBMP and Fe^{3+} was determined to be 1.0×10^{-4} M (Fig. 5b). A peak at 757.6 identified as the $[NIBMP-2H^{+}+Fe^{3+}+Cl+Cl+C_2H_5OH-OCH_3]$ ion was seen in the ESI-HRMS data of the generated 1 equivalent of NIBMP and 1 equivalent of $FeCl_3$ complex, which is shown in Fig. S3. This indicates that the binding stoichiometry between Fe^{3+} and NIBMP was 1:1.

Competitive binding studies

In order to assess the selectivity and appropriateness of NIBMP for real-world applications as a chemosensor towards Fe^{3+}, competitive studies were carried out in the presence of several metal ions (Na^{+}, Ca^{2+}, Fe^{2+}, Mn^{2+}, Fe^{3+}, Co^{2+}, Ni^{2+}, Cu^{2+}, Zn^{2+}, Cd^{2+}, Al^{3+}, Hg^{2+}, Sn^{2+}, Pb^{2+} and NO_3^{-}, PO_4^{3-}, CrO_4^{2-}, CO_3^{2-}, Cl^{-}, CH_3COO^{-}). No discernible variations in absorbance were found. It showed that even the

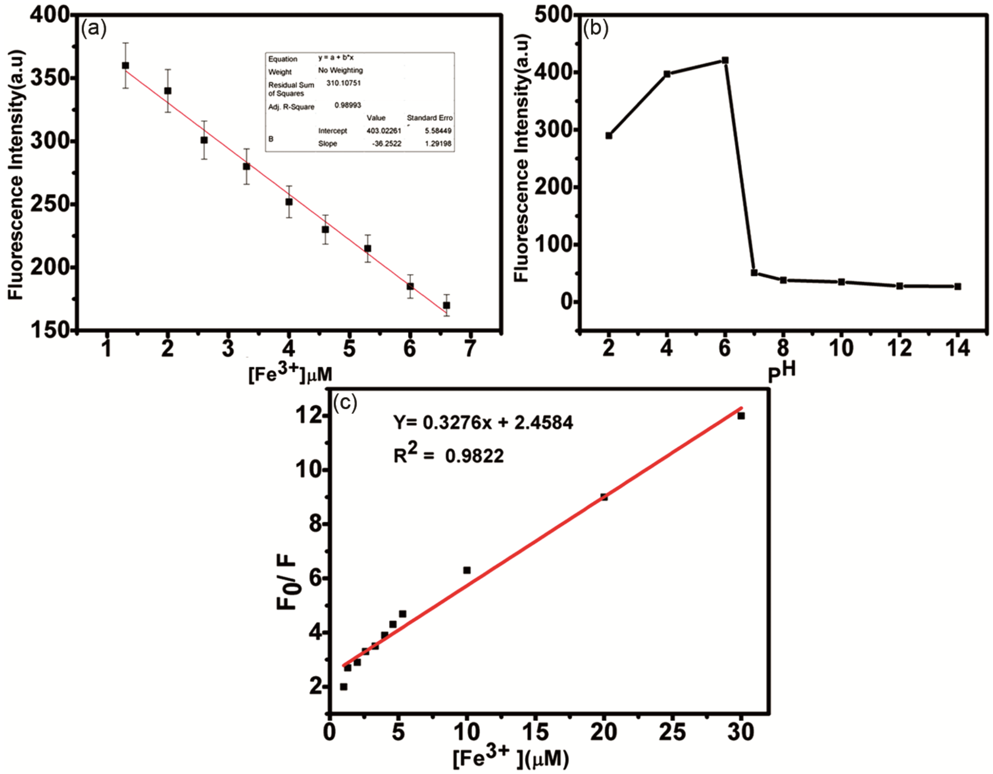

Fig. 4 — (a) Linear plot of fluorescence emission *vs* concentration of Fe^{3+} (b) Effect of *p*H on the fluorescence of NIBMP + Fe^{3+}(c) Stern –Volmer plot of fluorescence quenching of NIBMP with the addition Fe^{3+}

presence of other additional metal ions did not significantly affect the response of NIBMP towards Fe^{3+} (Fig. 5a).

Reversibility of EDTA

By including 1 mM EDTA, the quenching fluorescence intensity of NIBMP upon contact with Fe^{3+} was tested. The ejection of Fe^{3+} from the NIBMP+ Fe^{3+} complex was observed to increase the fluorescence intensity at 530 nm when EDTA was added to the complex. The addition of Fe^{3+} quenched the peak once more, this time at a slightly greater intensity, causing interaction with NIBMP that was chemically reversible (Fig. 5c). These tests on reversibility showed that NIBMP may be trusted as a source for monitoring Fe^{3+} in real time.

Sensing mechanism of NIBMP with Fe^{3+}

The probability of binding of Fe^{3+} with NIBMP is shown in Scheme 2. NIBMP emits yellow fluorescence under UV-light (365 nm). After excitation at 423 nm, NIBMP emitted fluorescence at 535 nm in the visible region with high intensity that was due to the presence of extensive conjugation and internal charge transfer (ICT) from –OH and OCH_3 of curcumin to azomethine. While complexing with Fe^{3+} *via* azomethine moiety (>C=N-), the fluorescence emission intensity of NIBMP was quenched, which might be attributed to the decrease in conjugation, internal charge transfer and the paramagnetic nature of Fe^{3+} with incomplete d shell withdraw the electrons from the >C=N- as a result internal charge transfer was inhibited[14]. The stochiometric ratio 1:1 and

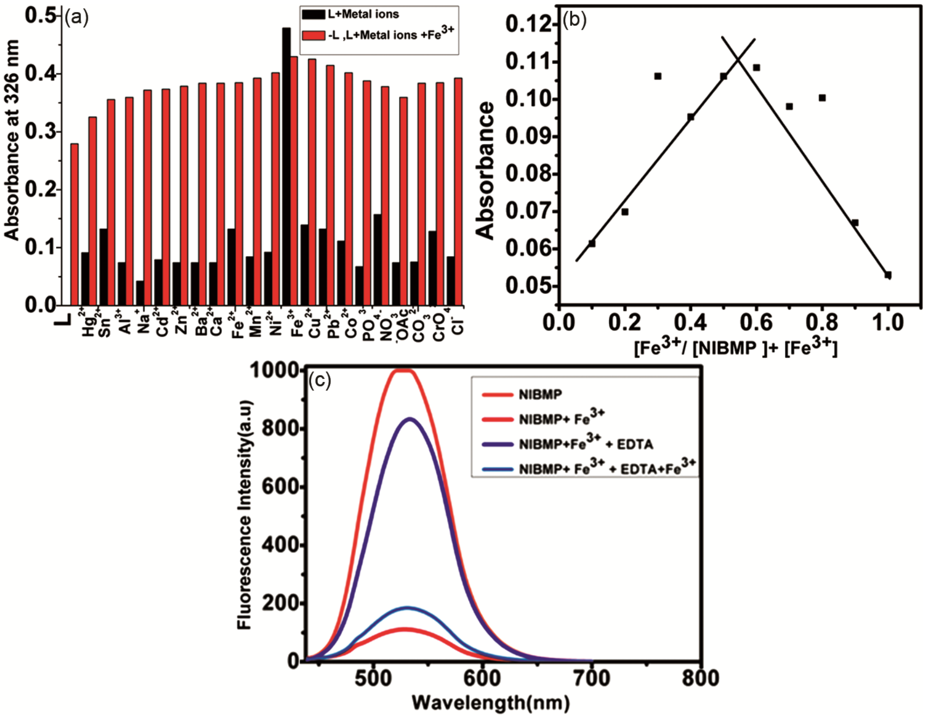

Fig. 5 — (a) Interference studies of various metal ions on Fe^{3+} (b) Job's plot of NIBMP with Fe^{3+} (c) Reversibility spectrum of NIBMP + Fe^{3+} with EDTA.

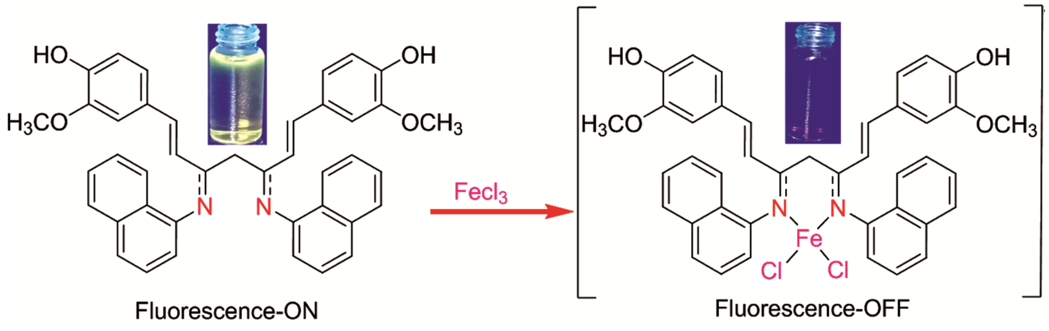

Scheme 2 — Proposed sensing mechanism of Fe^{3+} ion by NIBMP

Table 1 — Determination of Fe^{3+} in various water samples

Samples	Added (μM)	Found (μM)	Recovery (%)
Drinking water from our home	2	2.1017 ±0.001	105
Tap Water (From our Lab)	2	2.1321±0.001	106
Drinking water in our campus	2	2.0324 ±0.001	101

Table 2 — Comparison of lod of various Fe^{3+} colorimetric and fluorescent sensors

Probe	Method	LR	Lod	Ref. No.
Rhp	Colorimetric and fluorescent	0-50 μM	0.1023 μM	16
TSQ	Colorimetric	1-100 μM	1 μM	17
DN	Colorimetric and fluorescent	0-3.0 equiv.	0.178 μM	18
P1-AN	Colorimetric and fluorescent	10–50 mgL^{-1}	0.23 μM	19
Pyrazolo [3, 4h] Quinoline-3-Carbonitriles	Colorimetric and fluorescent	0-500 μM	0.86 μM	20
Phosphazene-based sensor	Fluorescent	4-30 μM	4.8 μM	21
Rhodamine–Phenylenediamine –bistriazole (RPBT)	Colorimetric & fluorescent	25-90 μM & 24-100 μM	5.0 μM 0.15 μM	22
PProDOTCB-salt	Colorimetric	20 –84 μM	23 μM	23
cyanoimidazopyridine-.based sensors (SS1 and SS2)	Colorimetric and fluorescent	0-100 equiv.	36.64 μM 14.33 μM	24
Quinoline Schiff base	Fluorescent	0–5.0 equiv.	0.048 μM	25
Curcumin Derivative	Colorimetric and fluorescent	0-10 μM	0.139 μM	Present work Schiff base

complexation was confirmed from Job' s plot analysis, HR-MS data (Fig. S3) and FT-IR spectrum of the complex (Fig. S5).

Real sample analysis

For the NIBMP, real sample investigations were conducted to evaluate its practical application in determining Fe^{3+}. The conventional addition technique was used to analyse several samples of water (including water from home and water collected on the campus of Thiagarajar College). Centrifuging and Whatman No. 1 filter paper were used to filter the obtained water samples. The levels of recovery were computed and shown in Table 1 after the water samples were added to the NIBMP and Fe^{3+} combination. The observed values were in the 101–106 range (percentage). In addition, the comparison of Lod of various Fe^{3+} colorimetric and fluorescent sensors are also summarised in Table 2. These findings showed that NIBMP could accurately detect the presence of Fe^{3+} and be applied in real-world settings.

Conclusions

We have developed a curcumin and 1-aminonaphthalene based colorimetric and fluorescence chemosensor (NIBMP) for the efficient and sensitive detection of Fe^{3+} ions. The colorimetric sensing investigation demonstrated that NIBMP allows for the "naked eye" detection of Fe^{3+} by a discernible colour shift from yellow to reddish-brown. Additionally, the ligand NIBMP preferentially detects Fe^{3+} over the other examined metal ions, according to absorption and emission analyses. According to Job's figure, the analysis of NIBMP binding to Fe^{3+} ions was determined to be 1:1. Fe^{3+} was discovered to have an NIBMP detection limit of 0.139 μM. By conducting interference investigations, it was further demonstrated that NIBMP is selective for Fe^{3+}. The examination of real samples demonstrated the usefulness of NIBMP for Fe^{3+}. Therefore, we anticipate that the findings of this work may aid in the creation of more multiple target chemosensors.

Supplementary Information

Supplementary information is available in the website http://nopr.niscpr.res.in/handle/123456789/58776.

References

1 Bhattacharya P T, Satya Ranjan Misra S R, & Hussain M, *Scientifica, (2016) 1–12.*
2 Tigineh G.T & Liu L.K, *Bull. Chem. Soc, Ethiop*, 31(2017) 31.
3 Jiang J, Gao P, Zhang Y, Zhang G, Zhou Y & Dong C, *Talanta,* 174 (2017) 44.
4 Robert C H & Xiole K, *Met. Ions Life Sci.* 13 (2013) 229.
5 Da En, Yuan G, Bo-Ting C, B Dong & Meng J P, *RSC Adv*. 4 (2014) 248.
6 Liang Y, Wang R, Liu G & Pu S, *ACS Omega,* 4 (2019) 6597.

7 Kim C, Min C, Na S, Shin J, Kim J & Jo T. G, *New J. Chem,* 41 (2017) 3991.

8 Sumathi S, Tharmaraj P, Sheela C D & Ebenezer R, *J. Coord. Chem*, 64 (2011) 1707.

9 Xu G, Wang J, Si G, Wang M, Xue X, Wu B & Zhou S, *Sens. Actuators B. Chem*, 230 (2016) 684.

10 Kareem A, Khan M S, Nami S A. A, Bhat S A, Mirza A U & Nishat N, *J. Mol. Struct,* 1167 (2018) 261.

11 Jayandran M, Haneefa M M & Balasubramanian V, *Indian J Sci. Technol*, 9 (2016) 1.

12 Kumar V, Singh A. K, Ganjali M. R, Norouzi P, Faridbod F & Mergu N, *Sens. Actuators B: Chem*, 182 (2013) 642.

13 Mondal A, Naskar B, Goswami S, Prodhan C, Chaudhuri K & Mukhopadhyay C, *Org. Biomol. Chem*, 16 (2018) 302.

14 Shylaja A, Roja S. S, Priya R. V & Kumar R. R, *J. Org. Chem,* 83 (2018) 14084.

15 Aydin Z & Keles M, *ChemistrySelect,* 5 (2020) 7375.

16 Liu X, Li N, Xu M. M, Wang J, Jiang C, Song G & Wang Y, *RSC Adv,* 8 (2018) 34860.

17 Shellaiah M, Thirumalaivasan N, Aazaad B, Awasthi K, Sun K W, Wu S P, Lin M C & Ohta N, *Spectrochim. Acta - Part A Mol. Biomol. Spectrosc,* 242 (2020) 118757.

18 Zuo Z, Song X, Guo D, Guo Z & Niu Q *J. Photochem. Photobiol. A Chem,* 382 (2019) 111876.

19 Nizar S A, Kobayashi T & Mohd Suah F B, *J. Lumin*. 35 (2020) 1286.

20 Maity P, Naskar B, Goswami S, Prodhan C, Chaudhuri T, Chaudhuri K & Mukhopadhyay C, *ACS Omega,* 3 (2018) 18646.

21 Kagit R, Yildirim M, Ozay O, Yesilot S & Ozay H, Inorg. Chem., 53 (2014) 2144.

22 Wechakorn K, Chomngam S, Eiamprasert U & Kongsaeree P, Chem.Pap.,75 (2020) 883.

23 Chen X, Zhao Q, Zou W, Qu Q & Wang F, *Sens. Actuators B. Chem*,244 (2017) 891.

24 Sasan S, Chopra T, Gupta A,Tsering D, Kapoor K.K & Parkesh R, *ACS Omega*,7(2022) 11114.

25 Li B, Tian J, Zhang D & Tian F, *Luminescence*, 32 (2017) 1567.